ICHEP'98 #219
Submitted to Pa 10
Pl 12

DELPHI 98-137 CONF 198
22 June, 1998

Updates of DELPHI results on searches with 189 GeV data

Preliminary

DELPHI Collaboration

Abstract

New results are presented, derived from the 189 GeV LEP run in 1998. These include searches for neutral and charged Higgs bosons, for charginos and sleptons in the MSSM framework and for neutralinos, gravitinos and stau in the GMSB scenario. Results from a search for FCNC are also presented.

Paper submitted to the ICHEP'98 Conference
Vancouver, July 22-29

1 Introduction

An update is presented of the DELPHI results on searches for new particles in e^+e^- interactions, including the preliminary new data at 189 GeV taken this year. The integrated luminosity recorded by the experiment is of approximately 34 pb^{-1} of which most has been used in the following analyses. Until now, no evidence was found for the production of new particles. The present data allow to improve the exclusion limits in the areas of the neutral, the invisible and the charged Higgs bosons, the charginos, the neutralinos and the sleptons in the MSSM framework and the neutralinos and the staus in the Gauge Mediated Supersymmetry Breaking (GMSB) scenario. The exclusion limit on FCNC in the decay of the top quark are also improved by including the 189 GeV data.

2 Search for Neutral Higgs Bosons

We have updated our search for neutral Higgs bosons described in [1] to include the data taken at 189 GeV. All eight channels used in the previous paper have been applied to the new data.

The analyses selections have been tuned to reflect the higher background from ZZ events at 189 GeV. The final working points have not been optimised, but are taken at the same efficiency as was used in 1997. The candidate Higgs masses, and background expectation from this latest data in the ZH channel after all selection criteria are shown in figure 2 and table 1 and 2.

channel	background	luminosity	events	signal
He^+e^-	$0.34^{+0.07}_{-0.06}$	33.2	0	0.16
$H\mu^+\mu^-$	0.48±0.08	31.9	0	0.23
$H\nu\bar{\nu}$	0.51±0.06	33.4	1	0.74
$Hq\bar{q}$	2.55±0.12	31.0	3	2.48
$(H \to q\bar{q})\tau^+\tau^-$	0.17±0.05	33.0	0	0.05
$(H \to \tau^+\tau^-)q\bar{q}$	0.73±0.11	33.0	0	0.12
$hA \to \tau^+\tau^- q\bar{q}$	0.17±0.05	33.0	0	0.05
$hA \to b\bar{b}b\bar{b}$	0.61±0.09	31.0	0	0.73

Table 1: Expected background, integrated luminosity, number of observed events and signal expectation in all channels. The number of signal events is given at 90 GeV/c^2 in the ZH search and 80 GeV/c^2 and $\tan\beta$= 20 in the hA .

The candidate event near the Z^0 mass is shown in figure 1. It has four distinct jets, and two detached secondary vertices were reconstructed in the jets of the Higgs candidate.

2.1 The SM Higgs boson

All results in this section are found using the data in combination with that taken at 183 GeV.

The compatibility of the observed data with the background hypothesis has been checked by finding the fraction of background-only experiments which have a smaller

channel	Mass	x_b
$\mathrm{Hq\bar{q}}$	91.5	2.0
$\mathrm{Hq\bar{q}}$	70.4	2.5
$\mathrm{Hq\bar{q}}$	68.7	1.9
$\mathrm{H}\nu\bar{\nu}$	62.8	0.9

Table 2: An overview of the candidates. x_b is the combined b-tagging variable used; all these candidates show significant evidence for b-quarks.

likelihood ratio for each putative Higgs mass. This is the CL_b shown in figure 3, where no statistically unlikely results can be seen. This is not surprising, as four candidates were found while the expected background was 4.8.

The confidence with which the SM Higgs boson can be excluded at each mass is calculated using $CL_s = CL_{sb}/CL_b$, which is shown in figure 4. The observed 95% CL lower limit on the mass, allowing for the errors on the background rates, is

$$m_{\mathrm{H}} > 89.6 \text{ GeV}/c^2$$

while the expected 95% CL lower limit is

$$m_{\mathrm{H}} > 89.5 \text{ GeV}/c^2$$

2.2 MSSM Neutral Higgs searches

No candidates are observed, while the expected background is 0.78. These results are combined with our data taken between 161 and 183 GeV.

The results translate into regions of the MSSM parameter space excluded at 95% CL. Except for m_{A} at low $\tan\beta$, they are not strongly dependent on the assumption about the mixing in the stop sector. The results are first presented in the (m_{h}, $\tan\beta$) plane in Figure 5. Whatever the assumption on the mixing, a 95% CL lower limit on m_{h} is derived for all values of $\tan\beta$ greater than or equal to unity:

$$m_{\mathrm{h}} > 77.5 \text{ GeV}/c^2$$

This limit arises from the performance of the searches at large $\tan\beta$, i.e. in the hA channel. The expected limit is 74.2 GeV/c^2. For the no mixing assumption, given that m_{h} is tightly constrained by the theory, all values of m_{A} are excluded in the low $\tan\beta$ region, providing a lower limit on $\tan\beta$:

$$\tan\beta > 2.2$$

The projection into the (m_{A}, $\tan\beta$) plane is shown in figure 6. We set a limit on m_{A} at:

$$m_{\mathrm{A}} > 78.3 \text{ GeV}/c^2$$

3 Search for invisible Higgs Bosons

This note presents an update to the search [2] for the channel $e^+e^- \rightarrow hZ$, with $Z \rightarrow q\bar{q}$ or $\mu^+\mu^-$ and the Higgs decaying into stable non-interacting particles rendering it invisible. The update considers a data sample corresponding to a luminosity of 27 pb^{-1} accumulated by DELPHI at 189 GeV centre of mass energy, in which the hadronic decay mode has been analyzed.

The analysis selection, constructed for the 183 GeV samples, has been reoptimized using the same procedure as before and based on the simulation samples generated at the new energy point. The simulation sets are analogous to the lower energy with the exception that `EXCALIBUR` [3] generator has been used to describe four-fermion final states.

3.1 Selections

Preselections were defined in three steps 'A', 'B' and 'C'. The agreement between the data and simulation was checked at each step. The preselection for multihadronic events (A) was kept unchanged compared to the 183 GeV analysis. The algorithm defining the selection for photon hermeticity (B) has been updated for improved efficiency and purity. The loose selections to define the signal region (C) have been tuned corresponding to the change in the centre of mass energy. The event selection using the iterated nonlinear discriminant method [4] was optimized in the same way as in the 183 GeV samples.

3.2 Selection results

The number of data events, the expected background and signal efficiencies in various steps of the selections are summarized in tables 3 and 4. The final selection consists of 10 data events, with an expected background of 12.0±0.6(stat.)±4.0(syst.). The relative systematic uncertainties are estimated conservatively to be the same as in the 183 GeV analysis.

The rates in data and simulation are in agreement, no structure is observed in the recoil mass distribution and the limits on the cross section and invisible Higgs mass computed at lower centre of mass energies can be updated.

Selection	Data	total MC	$q\bar{q}\gamma$	4-f	$\gamma\gamma$+bhabha
Step A	3982	3716±15	2400±1	442±1	740±42
Step B	3817	3461±2.4	2308±1	415 ±1	739±14
Step C	172	135.5±1.5	75.4±0.7	59.5±0.9	0.46± 0.24
1st IDA	22	26.3±0.8	8.6±0.3	22.6±0.7	0.0
final	10	12.0±0.6	1.0±0.1	11.0±.6	0.0

Table 3: $Hq\bar{q}$ channel: Data and simulated background rates after different steps of the analysis.

3.3 Limits

The observed and expected rates of events and their recoil masses in the working point selection were combined with the previous data sets in the two non-overlapping channels

Preselection	Efficiency [%] for different m_h (GeV/c^2)						
	60	65	70	75	80	85	90
Step A	96.1	97.7	97.4	96.2	97.4	97.6	96.2
Step B	88.3	89.8	89.8	89.5	90.3	90.2	89.3
Step C	73.0	74.5	75.4	72.4	74.4	75.3	69.4
1st IDA	64.8	65.5	68.0	66.5	69.5	70.5	64.0
final	45.9	49.8	53.7	53.9	57.9	57.0	49.1
±(stat.)	1.6	1.6	1.6	1.6	1.6	1.6	1.5
±(syst.)	4.6	5.0	5.3	5.3	5.8	5.7	4.9

Table 4: Hq$\bar{\text{q}}$ channel: Signal efficiencies after different steps of the analysis

Hq$\bar{\text{q}}$ at 161-183 GeV and H$\mu^+\mu^-$at the 183 GeV centre of mass energy.

Figure 7 displays the observed and expected upper limits on the cross section for the process $e^+e^- \rightarrow$ Z(anything)h(invisible) as function of the Higgs mass. From the comparison with the standard model Higgs cross section one finds for the observed (expected) mass limit 85.0 (85.5) GeV/c^2.

Using the DELPHI limits on the visible higgs cross section [1] and including the preliminary 189 GeV results a new lower mass limit of 84.3 GeV/c^2 is set, independent of the hypothesis on the fraction of invisible decay modes, as is apparent from figure 8. For the Majoron model the excluded region in the mixing angle versus Higgs mass plane is shown in figure 9.

4 Search for Charged Higgs Bosons

This is an update of the charged Higgs boson search described in paper [5]. An additional 27 pb^{-1} collected at a centre of mass energy of 189 GeV have been analysed using the same procedure as for the data collected at 183 GeV. The definition of the likelihood functions and the optimisation of the cut values have not been redone for the new data set. Thus, the same values for the data selection cuts as at 183 GeV have been used, except for the cases where the cut value scales with $\sqrt{s}$, in which case the scaled values have been used.

Tables 5–7 show the result of the analysis of the new data set and correspond to tables 1–3 at 183 GeV in the original paper.

Figure 10 shows the new observed exclusion limit for the charged Higgs boson obtained by including the new data set at 189 GeV, as well as the expected limit. Also shown is the previously observed exclusion limit obtained without the 189 GeV data. The agreement between the observed and expected limits with the new data set included is satisfactory. From the present analysis we conclude that the mass of the charged Higgs boson is greater than 59.2 GeV/c^2 for all values of the decay branching ratio of the charged Higgs boson.

Selection	Data	Total Bkg	W^+W^- Bkg	QCD Bkg	Efficiency H^+H^- (M_H=60 GeV/c^2)
Event preselection	289	299	195	104	0.82
4 Jets	148	165	121	44	0.55
ΔM and anti-b cut	59	62	53	9	0.30
$40 < M_{JJ} < 70$	16	12.9	8.4	4.5	0.25
Probability Cuts	3	4.0	2.6	1.4	0.17

Table 5: *Number of selected events and signal efficiency in the hadronic final state at different stages of the event selection procedure for $\sqrt{s}$ = 189 GeV.*

Selection	Data	Total Bkg	W^+W^- Bkg	QCD Bkg	Efficiency H^+H^- (M_H=60 GeV/c^2)
Event preselection	365	439	193	244	0.68
τ selection	148	182	108	72	0.54
$40 < M_{JJ} < 70$	20	25.6	11.7	13.1	0.41
Probability Cuts	2	1.89	1.46	0.43	0.31

Table 6: *Number of selected events and signal efficiency in the semi-leptonic final state at different stages of the event selection procedure for $\sqrt{s}$ = 189 GeV.*

5 Search for Charginos

An update of the searches for charginos and neutralinos is presented, based on a data sample corresponding to the 34.0 pb^{-1} recorded by the DELPHI detector in 1998, at a centre-of-mass energy of 189 GeV. The same selection criteria used at the centre-of-mass energy of 183 GeV are used here. Similar efficiencies are obtained. The detailed description of the analysis can be found in [6].

The total number of background events expected in the different topologies in the neutralino LSP scenario and in the gravitino LSP scenario is shown in tables 8 and 9, together with the number of events selected in the data. All the selected events are compatible with the expectation from the background simulation. As no evidence for a signal is found, exclusion limits are set.

Selection	Data	Total Bkg	W^+W^- Bkg	QCD Bkg	Efficiency H^+H^- (M_H=60 GeV/c^2)
Event preselection	132	128	18	94	0.57
Angular cuts	9	12.2	12.0	0.08	0.36
Energy cuts	3	5.8	5.5	0.06	0.27

Table 7: *Number of selected events and signal efficiency in the leptonic final state at different stages of the event selection procedure for $\sqrt{s}$ = 189 GeV.*

PRELIMINARY

E_{cm} = 189 GeV, $\mathcal{L}$ = 34 pb^{-1}

	Chargino channels (stable neutralino)					
	Non-degenerate selection			Degenerate selection		
Topology:	$jj\ell$	*jets*	$\ell\ell$	$jj\ell$	*jets*	$\ell\ell$
Obs. events:	0	10	5	3	4	1
Background:	0.68 ± 0.3	4.10 ± 0.4	5.61 ± 0.4	2.3 ± 0.5	3.0 ± 0.5	1.26 ± 0.3
Total:						
Obs. events:	15			8		
Background:	10.39 ± 0.6			6.56 ± 0.8		

Table 8: The number of events observed in data and the expected number of background events in the different chargino search channels under the hypothesis of a stable neutralino.

PRELIMINARY

E_{cm} = 189 GeV, $\mathcal{L}$ = 34 pb^{-1}

	Chargino channels (unstable neutralino)		
	Non-degenerate selection	Degenerate selection	Ultra-degenerate selection
Obs. events:	2	0	1
Background:	2.97 ± 0.4	0.52 ± 0.3	0.51 ± 0.1

Table 9: The number of events observed and the expected number of background events in the different ΔM cases under the hypothesis of an unstable neutralino.

5.1 Results in case of a stable neutralino

Fig. 11 shows the chargino production cross-sections as obtained in the MSSM at $\sqrt{s}$ = 189 GeV for different chargino masses for the non-degenerate and degenerate cases.

To derive the chargino mass limits, constraints on the process $Z \to \tilde{\chi}_1^0\tilde{\chi}_2^0 \to \tilde{\chi}_1^0\tilde{\chi}_1^0\gamma$ were also included. These were derived from the DELPHI results on single-photon production at LEP 1 [7].

The chargino mass limits are summarized in Table 10. The table also gives, for each case, the minimum excluded MSSM cross-section provided that $M_{\tilde{\chi}_1^\pm}$ is below the appropriate mass limit. These cross-section values are also displayed in Fig. 11.

The excluded region in the plane of neutralino mass versus chargino mass, assuming a heavy sneutrino, is shown in Fig. 12.

In the non-degenerate case with a large sneutrino mass (> 300 GeV/c^2), the lower limit for the chargino ranges between 93.5 GeV/c^2 (for a mostly higgsino-like chargino) and 91.2 GeV/c^2 (for a mostly wino-like chargino). The minimum excluded MSSM cross-section at $\sqrt{s}$ = 189 GeV is 1.0 pb, provided that $M_{\tilde{\chi}_1^\pm}$ is below 91.2 GeV/c^2.

In the degenerate case ($\Delta M = 5$ GeV/c^2), the cross-section does not depend significantly on the sneutrino mass, since the chargino is higgsino-like under the assumption of gaugino mass unification. The lower limit for the chargino mass, shown in Fig. 11, is

89.9 GeV/c^2. The minimum excluded MSSM cross-section is in this case 1.22 pb.

A lower limit of 30.6 GeV/c^2 on the lighest neutralino mass is then obtained assuming $M_1/M_2 \gtrsim 0.5$, valid for $\tan\beta \geq 1$ and a sneutrino mass > 300 GeV/c^2, using the obtained chargino exclusion regions and including the DELPHI results [7] on the process $Z \to \tilde{\chi}_1^0\tilde{\chi}_2^0 \to \tilde{\chi}_1^0\tilde{\chi}_1^0\gamma$. The lower mass limit is obtained for $\tan\beta = 1$, μ = -60.52 GeV/c^2, M_2 = 51.38 GeV/c^2. Fig. 12 shows the limit on $M_{\tilde{\chi}_1^0}$ in the ($M_{\tilde{\chi}_1^\pm}$,$M_{\tilde{\chi}_N^0}$) plane.

5.2 Results in case of an unstable neutralino

The chargino cross-section limits corresponding to the case where the neutralino is unstable and decays via $\tilde{\chi}_1^0 \to \tilde{G}\gamma$ are computed as explained in section 5.1 and they are shown in Fig.11, and in table 10. In the non-degenerate case the chargino mass limit at 95% confidence level is 93.6 GeV/c^2 for a heavy sneutrino, while in the ultra-degenerate case ($\Delta M = 1$ GeV/c^2) the limit is 93.7 GeV/c^2. The minimum MSSM cross-section excluded by the above mass limits are 0.41 pb in the non degenerate case and 0.37 pb in the ultra-degenerate case.

PRELIMINARY

E_{cm} = 189 GeV, $\mathcal{L}$ = 34 pb^{-1}

Case	$m_{\tilde{\nu}}$ (GeV/c^2)	$M_{\chi^\pm}^{min}$ (GeV/c^2)	σ^{max} (pb)	$N_{95\%}$
Stable neutralino				
$\Delta M > 10$ GeV/c^2	> 300	91.2	1.0	15.4
$\Delta M = 5$ GeV/c^2	> 41	89.9	1.22	9.2
Unstable neutralino				
$\Delta M > 10$ GeV/c^2	> 300	93.6	0.41	4.58
$\Delta M = 1$ GeV/c^2	> 41	93.7	0.37	4.35

Table 10: 95 % confidence level limits for the chargino mass, the corresponding pair production cross–sections limits at 189 GeV and the 95 % confidence level upper limit on number of observed events, for the non–degenerate and a highly degenerate cases, in the "Neutralino LSP" and "Gravitino LSP" scenarios. The limits apply for a heavy sneutrino ($m_{\tilde{\nu}} > 300$ GeV/c^2).

6 Search for Scalar Leptons

The data collected by DELPHI during 1998 has been used to search for staus. This data-set corresponds to an integrated luminosity of 34 pb^{-1}. The event selection cuts were identical to the analysis of the data collected in 1997 at $E_{cms} = 183$ GeV [8].

The selection efficiency for the stau signal was estimated by using the same cut values as obtained for $E_{cms} = 183$ GeV. To verify this assumption, an efficiency scan was performed for an LSP mass of 20 GeV/c^2 at $E_{cms} = 189$ GeV. It is found that the dependence on the stau mass of the efficiency closely follows that at the lower E_{cms}, but with a slight shift to lower values. This shift was 3 %, and was applied as an over-all reduction at all points in the mass-plane when calculating the excluded area.

Seven candidates were found, with a total background of 6.10 ± 0.49 events. Of this number, 0.93 events from $\gamma\gamma$ interactions were considered as un-subtractable background when calculating the exclusion region. The break-down of the background in different channels is given in table 11. The excluded region for a righthanded stau combining all data collected by DELPHI at 130, 136, 161, 172, 183, and 189 GeV is shown in figure 13. One observes that by including the data at 189 GeV, the obtained limit increases by around 3.5 GeV/c^2 at large mass differences, while the expected limit increases by 4.5 GeV/c^2 in the same region.

4 fermion events	4.42 ± 0.44
$Z/\gamma \to \tau^+\tau^-$	0.55 ± 0.14
$Z/\gamma \to q\bar{q}$	0.05 ± 0.03
$\gamma\gamma \to e^+e^-, \mu^+\mu^-, \tau^+\tau^-$	0.93 ± 0.15
Total	6.10 ± 0.49
Events observed	7

Table 11: Expected background from different sources.

7 Study of single photon events

The energy spectrum and recoil mass distribution of the single-photon events collected at $\sqrt{s} = 189$ GeV have been studied in the polar-angle regions $13^\circ < \theta_\gamma < 32^\circ$ (forward) and $45^\circ < \theta_\gamma < 88^\circ$ (barrel). The total integrated luminosity of the analysed sample amounts to 26.5 pb^{-1}. Only photons with measured energy greater than 6 GeV were considered. The detailed description of the selection requirements applied to the data can be found in [9]. The photon energy spectrum and the recoil mass distribution of the selected events are shown in Figure 14, where they are compared with the main Standard Model background of $e^+e^- \to \nu\overline{\nu}\gamma$ events as simulated with the KORALZ [10] generator.

8 Search for new physics in events with photons and missing energy

Pairs of photons with missing energy are expected from reactions like $e^+e^- \to YY$ with the subsequent decay $Y \to X\gamma$, where X is a neutral undetected particle. Such processes are expected in supersymmetric models with gauge-mediated supersymmetry breaking (GMSB) [11, 12, 13, 14, 15], where the Y particle can be the lightest neutralino ($\tilde{\chi}_1^0$) decaying to a photon and a gravitino ($\tilde{G}$), and in more conventional SUSY models [16, 17] with $\tilde{\chi}_1^0$-LSP, where the Y and X are identified with $\tilde{\chi}_2^0$ and $\tilde{\chi}_1^0$ respectively. The main Standard Model background consists of $e^+e^- \to \nu\overline{\nu}\gamma\gamma(\gamma)$ events.

This section describes an update of the search for anomalous production of photon pairs with missing energy already applied to the data collected at lower centre-of-mass energies [18]. The data considered in this update are those collected by the DELPHI detector at the centre-of-mass energy of 189 GeV, corresponding to a total integrated luminosity of 25 pb^{-1}. All the results presented here are very preliminary.

As for the previous analyses the search is based on a two-step procedure:

- First events with two energetic photons and missing transverse energy are selected. This preselection is used in order to monitor the modelling of the Standard Model process $e^+e^- \to \nu\overline{\nu}\gamma\gamma(\gamma)$ which dominates the expected background.
- In a second step the signal is enhanced over the background by requirements for missing mass, transverse momentum or polar angle. The cuts involved in this second step depend on the assumption about the X particle, which can be extremely light (as in the case of the gravitino in GMSB models) or relatively heavy (as the $\tilde{\chi}_1^0$ in the SUSY scenario considered in [17]).

8.1 Event preselection

Year	$\sqrt{s}$ (GeV)	$\int \mathcal{L}$ (pb^{-1})	Data	$e^+e^- \to \nu\overline{\nu}\gamma\gamma(\gamma)$
1995	130	2.92	0	0.73±0.02
1995	136	3.01	0	0.70±0.02
1996	161	9.58	1	1.39±0.03
1996	172	9.85	3	1.09±0.03
1997	130	3.05	0	0.77±0.02
1997	136	2.91	0	0.68±0.02
1997	183	49.73	6	4.78±0.12
1998	189	26.50	3	2.35±0.21
Total	130-189	107.55	13	12.49±0.30

Table 12: The year of data taking, the centre-of-mass energy, the integrated luminosity, the number of events passing the preselection of two-photon events with missing energy and the number of background events expected in the Standard Model.

In the data sample analysed three events pass the preselection requirements. The background expected from the $e^+e^- \to \nu\overline{\nu}\gamma\gamma(\gamma)$ process amounts to 2.35 events at $\sqrt{s} =$

189 GeV according to the KORALZ model [10]. The contribution of the other background sources has been estimated to be negligible.

In Figure 15 the missing mass distribution is compared with the KORALZ expectations. Table 12 summarises the number of events found and expected from the background at the various centre-of-mass energies. A good agreement is found between the observed data and the background simulation. Summing up all data samples, 13 events were found, while 12.5 events were expected from the Standard Model background.

$\sqrt{s}$ (GeV)	Run/Event	$E_{\gamma 1}$ (GeV)	$E_{\gamma 2}$ (GeV)	$\theta_{\gamma 1}$ (°)	$\theta_{\gamma 2}$ (°)	M_{miss} (GeV/c^2)	$M_{\tilde{\chi}_1^0}^{max}$ (GeV/c^2)
189	83889/3889	73.1	8.4	105.9	123.1	73.7	66.6

Table 13: The relevant features (photon energies, photon polar angles and missing mass) of the candidate events found in the search for the reaction $e^+e^- \to YY \to X\gamma X\gamma$, in the case of a massless X particle.

$\sqrt{s}$ (GeV)	Data	$e^+e^- \to \nu\overline{\nu}\gamma\gamma(\gamma)$
130	0	0.17±0.01
136	0	0.15±0.01
161	0	0.36±0.02
172	2	0.33±0.02
183	0	1.65±0.08
189	1	0.89±0.12
Total	3	3.55±0.11

Table 14: The number of candidates found in the data and expected from the $e^+e^- \to \nu\overline{\nu}\gamma\gamma(\gamma)$ background as a function of the centre-of-mass energy. The results correspond to the search for the reaction $e^+e^- \to YY \to X\gamma X\gamma$ where the X particle is practically massless.

8.2 Case of massless X particles

One event was found in the data taken at $\sqrt{s} = 189$ GeV passing the final selection for the $m_X \approx 0$ case. The event features are described in Table 13. The background expected from Standard Model processes amounts to 0.9 events. The maximum Y mass compatible with the features of the selected candidate is 66.6 GeV/^{2}.

The number of detected events at each centre-of-mass energy are summarised in Table 14, together with the corresponding background estimates. No excess of events was found in the data.

8.3 Case of massive X particles

In the analysis optimised for a massive X particle, one event was found while 0.9 were expected from the background simulation. This candidate is the same as the one selected in the massless X case and is described in the previous section. The distribution of the various data candidates among the centre-of-mass energies are described in Table 15.

$\sqrt{s}$ (GeV)	Data	$e^+e^- \to \nu\overline{\nu}\gamma\gamma(\gamma)$
130	0	0.38±0.02
136	0	0.35±0.02
161	0	0.45±0.03
172	1	0.36±0.02
183	3	1.85±0.09
189	1	0.93±0.12
Total	5	4.32±0.13

Table 15: The number of candidates found in the data and expected from the $e^+e^- \to \nu\overline{\nu}\gamma\gamma(\gamma)$ background as a function of the centre-of-mass energy. The results correspond to the search for the reaction $e^+e^- \to YY \to X\gamma X\gamma$ where the X particle is massive.

8.4 Limits on the signal cross-section

Since no evidence for a signal was found in the data, cross-section limits for the process $e^+e^- \to YY$, followed by $Y \to X\gamma$, were derived for each considered centre-of-mass energy and any X,Y mass combination.

The cross-section limits have been calculated at $\sqrt{s} = 189$ GeV using the 1998 data sample separately and combined with the other data samples collected at lower centre-of-mass energies. The combined limit was obtained with the Likelihood ratio multichannel method. The cross-section limits are shown in Figure 16 and in Figure 17.

9 Search for single-photon events with the photon not coming from the interaction region

A search for single-photon events in which the photon shower axis, as reconstructed in the HPC calorimeter, does not point at the beam interaction region has been performed on the data collected at $\sqrt{s} = 189$ GeV. Events of this kind are not expected in the Standard Model (apart from those produced by the finite angular resolution of the HPC shower reconstruction algorithm).

In the framework of Gauge-Mediated SUSY Breaking models (GMSB) [11, 12, 13, 14, 15] such events could be the signature for neutralino pair-production followed by the subsequent decay $\tilde{\chi}_1^0 \to \tilde{G}\gamma$ with relatively long lifetime.

The selection criteria considered in this update are identical to those applied to the data taken at lower centre-of-mass energies and described in [18]. The basic requirement

for this search is a cut rejecting events with reconstructed shower impact parameter smaller than 40 cm with respect to the beam spot.

No candidates were observed in the 1998 data sample, corresponding to an integrated luminosity of 26.5 pb^{-1}, while 0.1 events were expected on the basis of the Monte Carlo simulation of the $\mathrm{e^+e^-} \to \nu\overline{\nu}\gamma$ background process.

10 Search for Neutralinos in light gravitino scenarios with $\tilde{\tau}$ NLSP

This search, described in [19] of this conference, was updated for a luminosity of $\sim 34 pb^{-1}$ at $\sqrt{s} = 189$ GeV. If produced, each lightest neutralino ($\tilde{\chi}_1^0$) would promptly decay into a stau ($\tilde{\tau}$) and a τ. It is assumed that staus decay promptly through the reaction $\tilde{\tau} \to \tau\tilde{G}$, where $\tilde{G}$ is a gravitino. These last particles are, for the effects of kinematics, massless. R-parity is assumed to be conserved, implying that $\tilde{G}$s escape the detector undetected. Thus, the final topology searched for consists of four τs and missing energy.

The analysis described in [19] was not modified. The cuts in the analysis are:

- Cuts against $\gamma\gamma$ backgrounds: which include cuts on the transverse energy, the energy in a cone of 30° around the beam axis and the missing mass. After these cuts, the $\gamma\gamma$ background is reduced by a factor of the order of 30.

- Cuts against $\mathrm{f\bar{f}}(\gamma)$ backgrounds: by imposing a maximum number of good tracks, a cut on the thrust, on the two jet acoplanarity and on the minimum missing mass of the events After these cuts, the $\mathrm{f\bar{f}}(\gamma)$ background was reduced by a factor of the order of 15.

- Cuts based on topology: signal events tend naturally to cluster into a 4-jet topology. All jets should be away from the beam-pipe direction. When reduced by the jet algorithm into a 2-jet configuration, each of these jets should be broader than 20° and well separated from each other.

The expected background for 34 pb^{-1} at $\sqrt{s} = 189$ GeV, is 0.33 events. No candidates were found in the data sample. Thus, new lower limits on production cross section and neutralino masses can be derived.

We follow the same model [20] as in reference [19]. This is a general model with only the assumptions of radiative electroweak symmetry breaking and null trilinear couplings at the messenger scale. The corresponding parameter space was scanned as follows: $1 \leq n \leq 4$, 5 TeV $\leq \Lambda \leq$ 900 TeV, $1.1 \leq M/\Lambda \leq 9000$, $1.1 \leq \tan\beta \leq 50$, and $sign(\mu) > 0$. n is the number of messenger generations in the model, Λ is the ratio between the vacuum expectation values of the auxiliary component superfield and the scalar component of the superfield and M is the messenger mass scale; $\tan\beta$ and μ are defined as for the MSSM.

Figure 18 shows the new excluded regions in the $(m_{\tilde{\tau}_1}, m_{\tilde{\chi}_1^0})$ space. Two other analyses are taken into account. The first is the search for lightest neutralino pair production in the region of the parameter space where $\tilde{\chi}_1^0$ is the NLSP [21]. Within this scenario, the neutralino decays into a gravitino and a photon. The second is the search for $\tilde{\tau}_1$-pair production in the context of the MSSM. In the case where the MSSM $\tilde{\chi}_1^0$ is massless, the

kinematics correspond to the case of $\tilde{\tau}_1$ decaying into a τ and a gravitino, except for spin effects, which are not taken into account in SUSYGEN.

Figure 18 shows the 95% C.L. excluded areas for the case $n = 2$ and gaugino-like neutralinos in the $m_{\tilde{\chi}_1^0}$ *vs.* $m_{\tilde{\tau}_1}$ plane. The positive-slope dashed area is excluded by this analysis. The resulting 95% C.L. lower limit on the mass of the lightest neutralino is 83 GeV/c^2. The negative-slope dashed area is excluded by the analysis searching for neutralino-pair production followed by the decay $\tilde{\chi}_1^0 \to \tilde{G}\gamma$. The pointed area is excluded by the direct search for MSSM $\tilde{\tau}_1$-pair production [8], taking into account the possibility of $\tilde{\tau}_L - \tilde{\tau}_R$ mixing [22].

11 Search for Flavour Changing Neutral Currents

A search for Flavour Changing Neutral Currents (FCNC) has been performed using data taken at the center of mass energy of 189 GeV in the reaction $e^+e^- \to \bar{t}c + \bar{t}u$ + CC.

Performing the same analysis as at $\sqrt{s} = 183$ GeV in hadronic W decays one gets an estimated background of 2 events while 1 event was observed in real data. The estimated efficiency is of 0.15.

The resulting upper limit at 90% confidence level on the cross section is 0.6 pb for the 189 GeV data alone.

Run	Channel	Limit
183 GeV	hadrons + $l\nu$	<0.4 pb
189 GeV	hadrons	<0.6 pb

Table 16: Upper limits on the cross-section.

The cross section for FCNC processes depends on the top-quark mass due to the threshold behaviour of the cross-section in this region. To compare with the CDF results, the limit on the cross-section corresponding to the process $Z \to t\bar{c}+t\bar{u}$ has been converted into a limit on the branching ratio $Br(t \to Zc) + Br(t \to Zu)$ as a function of m_t. The earlier DELPHI result at 183 GeV as well as the 183+189 GeV combined result are displayed in figure 19. One can see that the CDF limit is reached for the lowest possible experimental value of the t-quark mass.

References

[1] DELPHI Collaboration, W. Adam *et al.*, DELPHI 98-95 CONF 163 and Paper #200 submitted to ICHEP'98.

[2] DELPHI Collaboration, P. Abreu et al., DELPHI 98-126 CONF 187 and Paper #218 submitted to ICHEP'98.

[3] F.A. Berends, R. Pittau and R. Kleiss, Comp. Phys. Comm. **85** (1995) 437.

[4] T.G.M. Malmgren, Comp. Phys. Comm. 106 (1997) 230;
T.G.M. Malmgren and K.E. Johansson, Nucl. Instr. and Meth. 403 (1998) 481.

[5] DELPHI Collaboration, M. Battaglia, T. Ekelöf, M. Ellert, A. Kiiskinen, V. Ruhlmann Kleider, S. Stanič, DELPHI 98-96 CONF 164 and Paper #214 submitted to ICHEP'98.

[6] DELPHI Collaboration, P. Abreu *et al.*., Eur. Phys. J. **C1** (1998) 1;
DELPHI Collaboration, P. Anderson, I. Gil, A. Lipniacka, S. Navas, P. Rebecchi, K. Hultqvist, DELPHI 98-66 CONF 134 and Paper #201 submitted to ICHEP'98.

[7] DELPHI Collaboration, P. Abreu *et al.*, Z. Phys. **C74** (1997) 577

[8] DELPHI Collaboration, W. Adam *et al.*, DELPHI 98-92 CONF 160 and Paper #204 submitted to ICHEP'98.

[9] P. Checchia et al., DELPHI 98-7 PHYS 758.

[10] S. Jadach et al., Comp. Phys. Comm. **66** (1991) 276.

[11] P. Fayet, Phys. Lett. **B69** (1977) 489;
P. Fayet, Phys. Lett. **B70** (1977) 461.

[12] J. Ellis and J.S. Hagelin, Phys. Lett. **B122** (1983) 303.

[13] S. Ambrosanio et al., Phys. Rev. **D54** (1996) 5395.

[14] S. Dimopoulos et al., Phys. Rev. Lett. **76** (1996) 3494;
S. Dimopoulos et al., Phys. Rev. **D54** (1996) 3283.

[15] S. Dimopoulos, S. Thomas and J.D. Wells, Nucl. Phys. **B488** (1997) 39.

[16] S. Ambrosanio et al., Phys. Rev. Lett. **76** (1996) 3498;
S. Ambrosanio et al., Phys. Rev. **D55** (1997) 1392;
H.E. Haber and D. Wyler, Nucl. Phys. **B323** (1989) 267.

[17] G.L. Kane and G. Mahlon, Phys. Lett. **B408** (1997) 222.

[18] DELPHI Collaboration, DELPHI 98-69 CONF 147 and Paper #207 submitted to ICHEP'98.

[19] G. Wolf, R. Alemany, C. Garcia, F.R. Cavallo, F.L. Navarria, DELPHI Collaboration, DELPHI 98-68 CONF 136 and Paper #205 submitted to ICHEP'98.

[20] D. A. Dicus, B. Dutta, S. Nandi, Phys. Rev. **D56** (1997) 5748;
D. A. Dicus, B. Dutta, S. Nandi, Phys. Rev. Lett. **78** (1997) 3055.

[21] DELPHI Note 98-7 PHYS 758.

[22] A. Bartl *et. al.*, Z. Phys. C73(1997) 469.

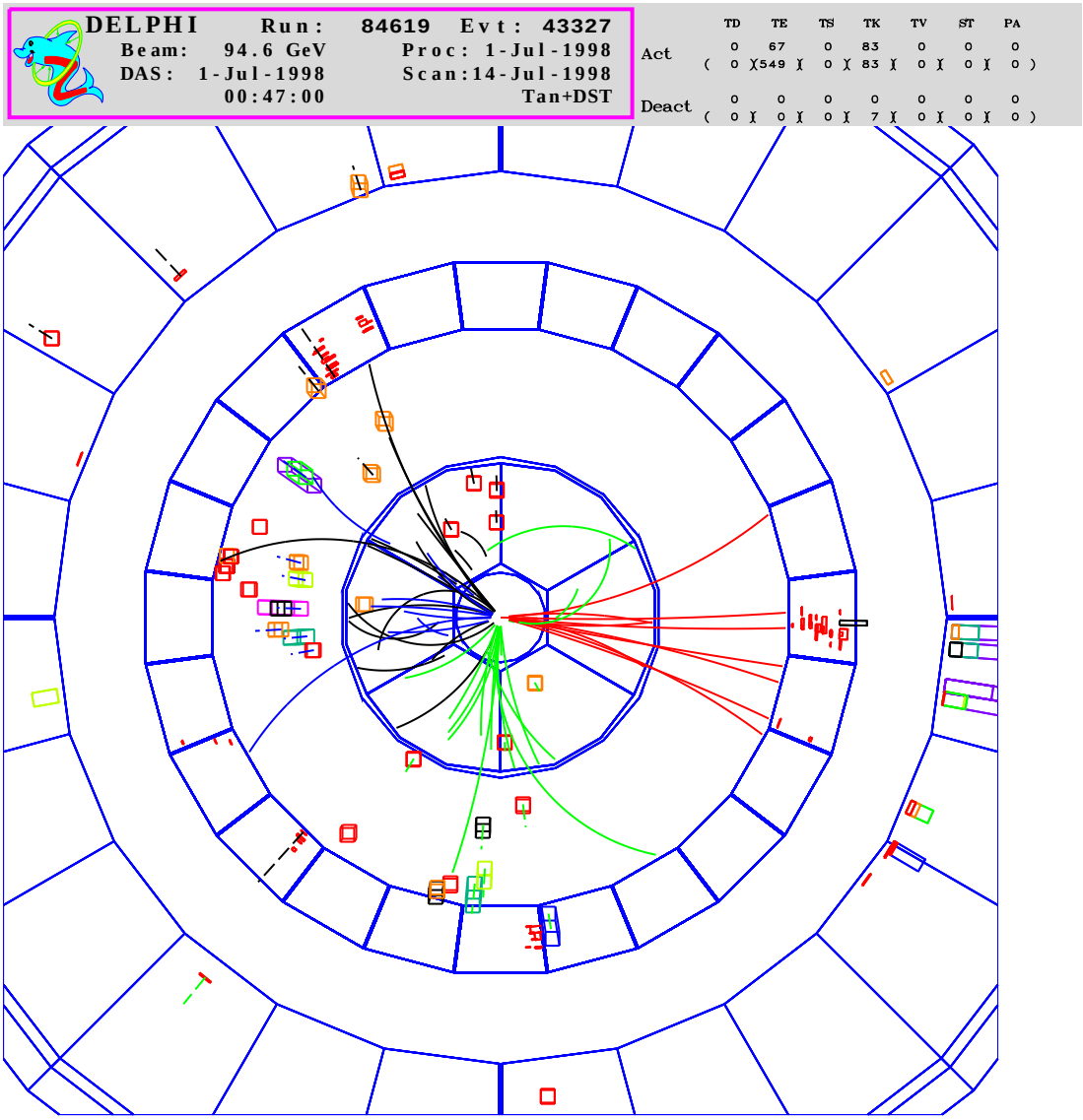

Figure 1: A Higgs candidate found in the four jet search. The putative Higgs mass is 91.5 GeV/c^2.

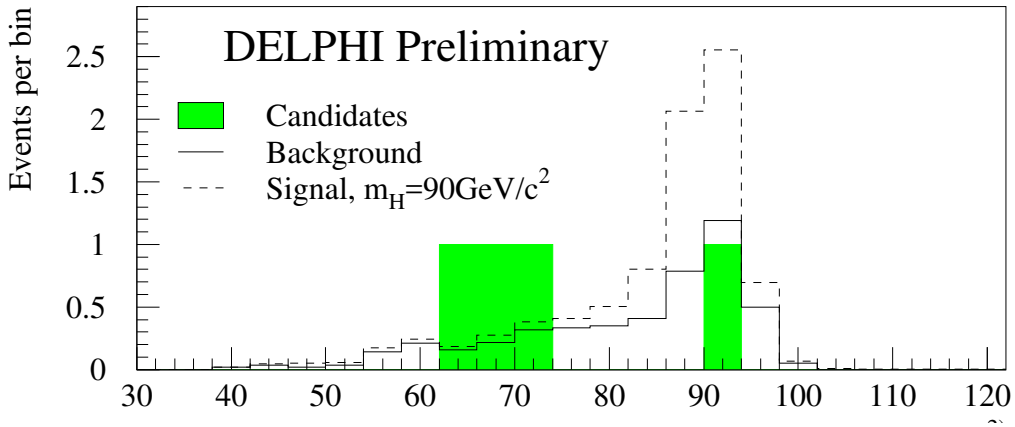

Figure 2: Final distribution of the reconstructed candidate masses when combining all ZH analyses at 189 GeV. Data are compared with (normalised) background expectations. The expectation from a signal at 90 GeV/c^2 is also shown. All background sources are summed.

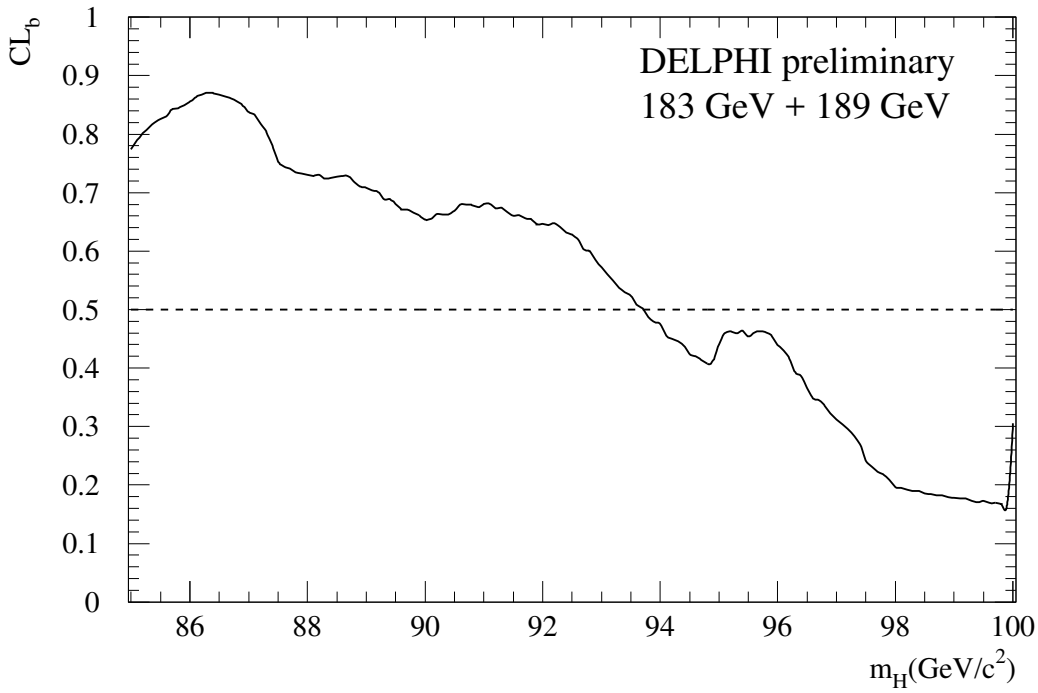

Figure 3: Confidence level in the background hypothesis as a function of the SM Higgs boson mass. Curves are shown for the expected (dotted) and observed (solid) confidences.

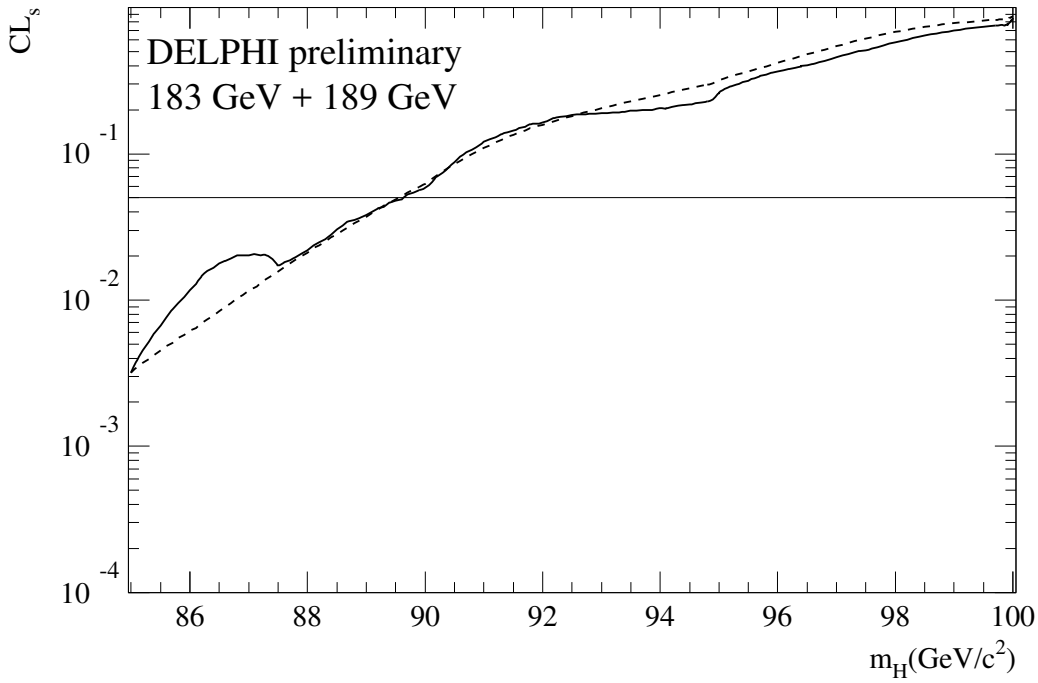

Figure 4: Confidence level in the signal hypothesis as a function of the SM Higgs boson mass. Curves are shown for the expected (dashed line) and observed (solid line) confidence levels. The intersections of the horizontal lines at 5% with the curves define the expected and observed 95% CL lower limits on the Higgs boson mass. These results incorporate our previous results at 183 GeV.

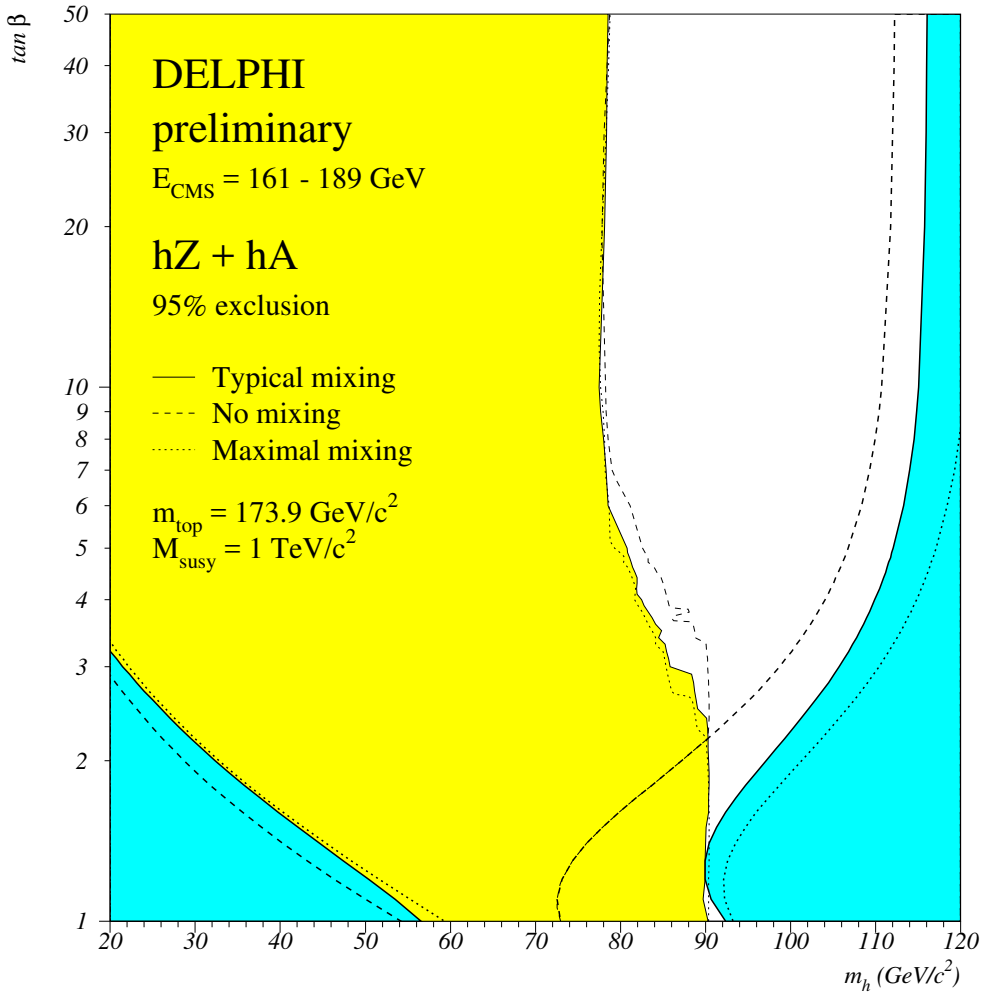

Figure 5: Regions in the ($m_{\rm h}$, $\tan\beta$) plane excluded at 95% CL by the searches in the ZH and hA production modes at $\sqrt{s}$ =133 to 189 GeV. Three hypotheses for the mixing in the stop sector have been considered. The regions not allowed by the MSSM model for a top mass of 175 GeV/c^2 and a SUSY scale of 1 TeV are also indicated (in dark grey for the typical mixing).

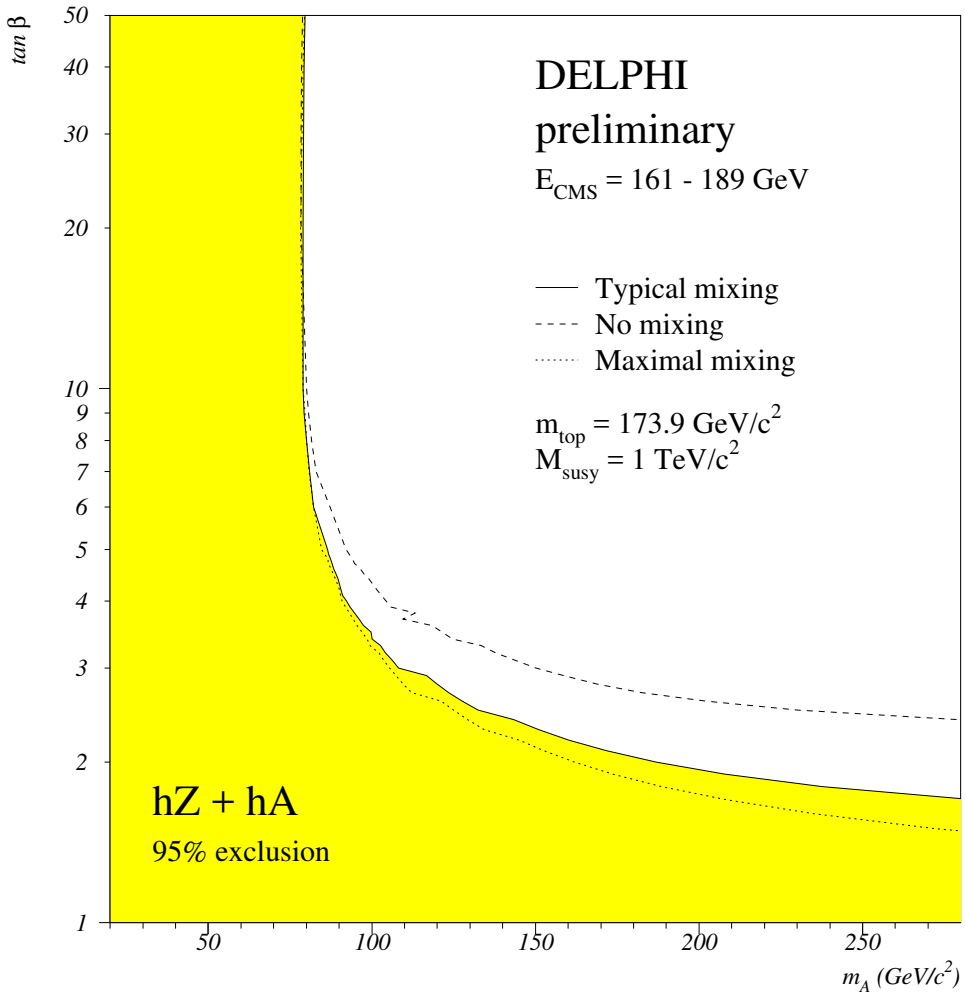

Figure 6: Region in the (m_{A}, tan β) plane excluded at 95% CL by the result of the searches in the ZH and hA channels at $\sqrt{s}$ =133 to 189 GeV. Three different hypotheses for the mixing in the stop sector are presented.

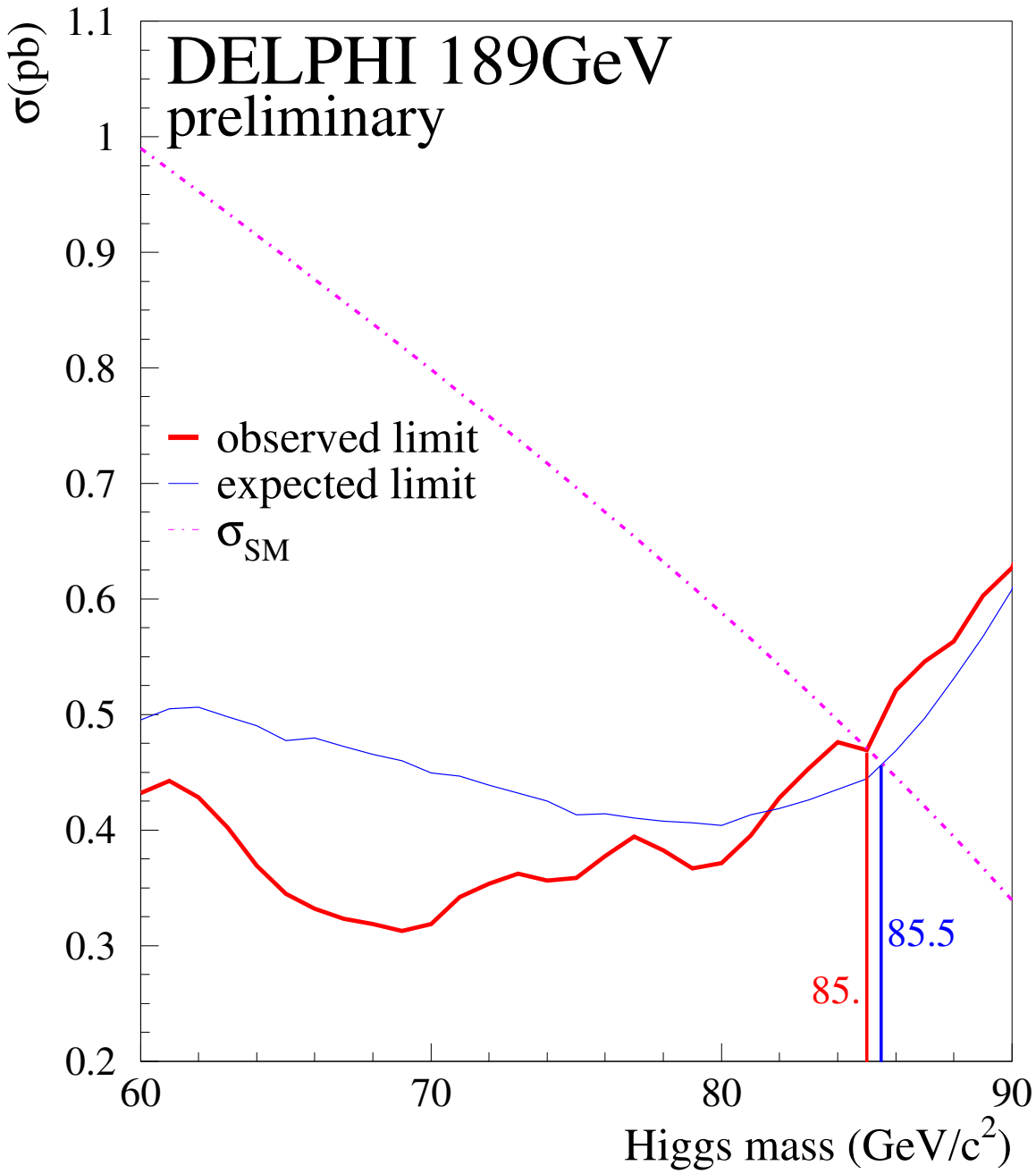

Figure 7: The 95 % confidence level upper limit on the cross section $e^+e^- \rightarrow$ Z (anything) h(invisible) as a function of the Higgs boson mass.

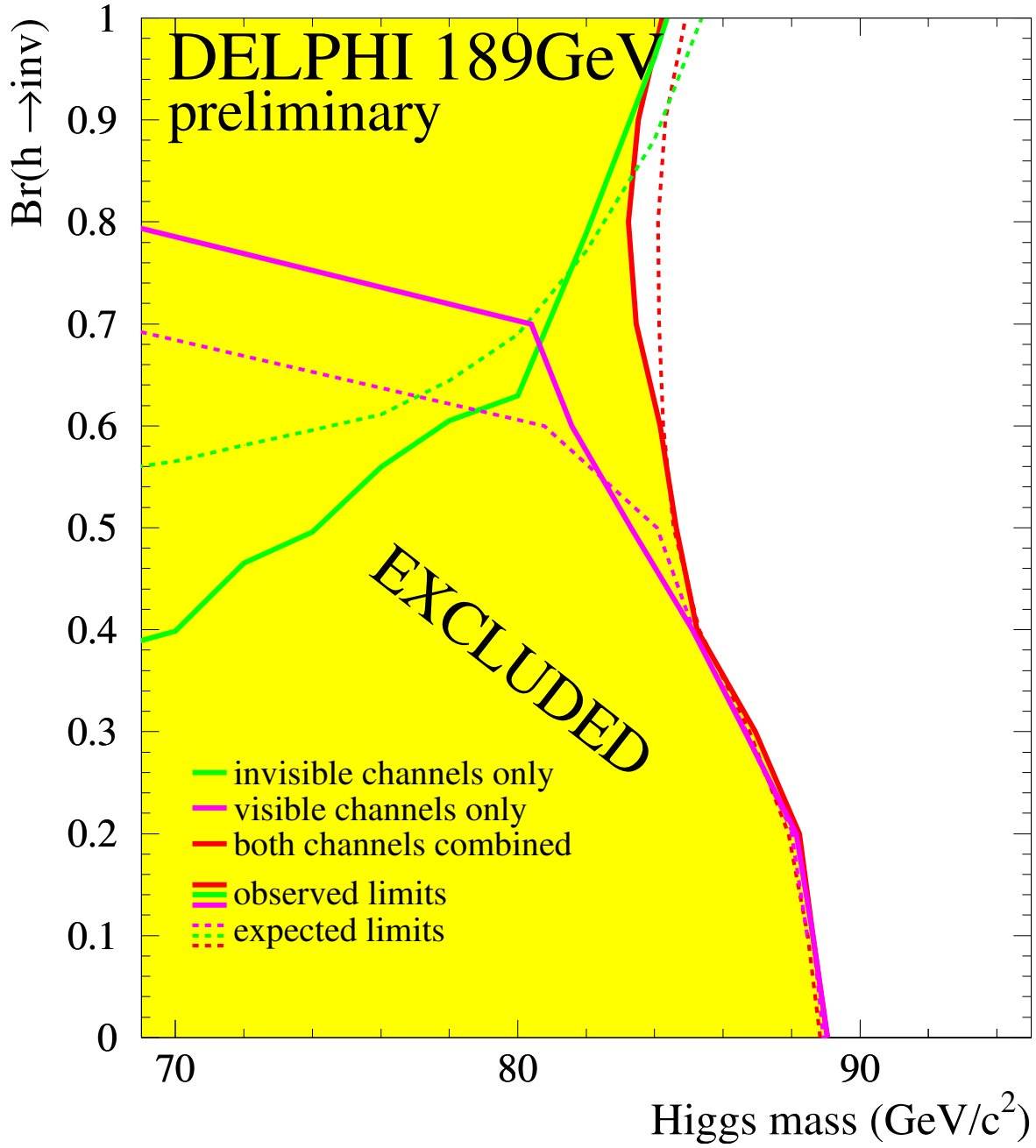

Figure 8: The excluded Higgs limits as function of the branching ratio into invisible decays BR, assuming a $1 - BR$ branching ratio into standard visible decay modes.

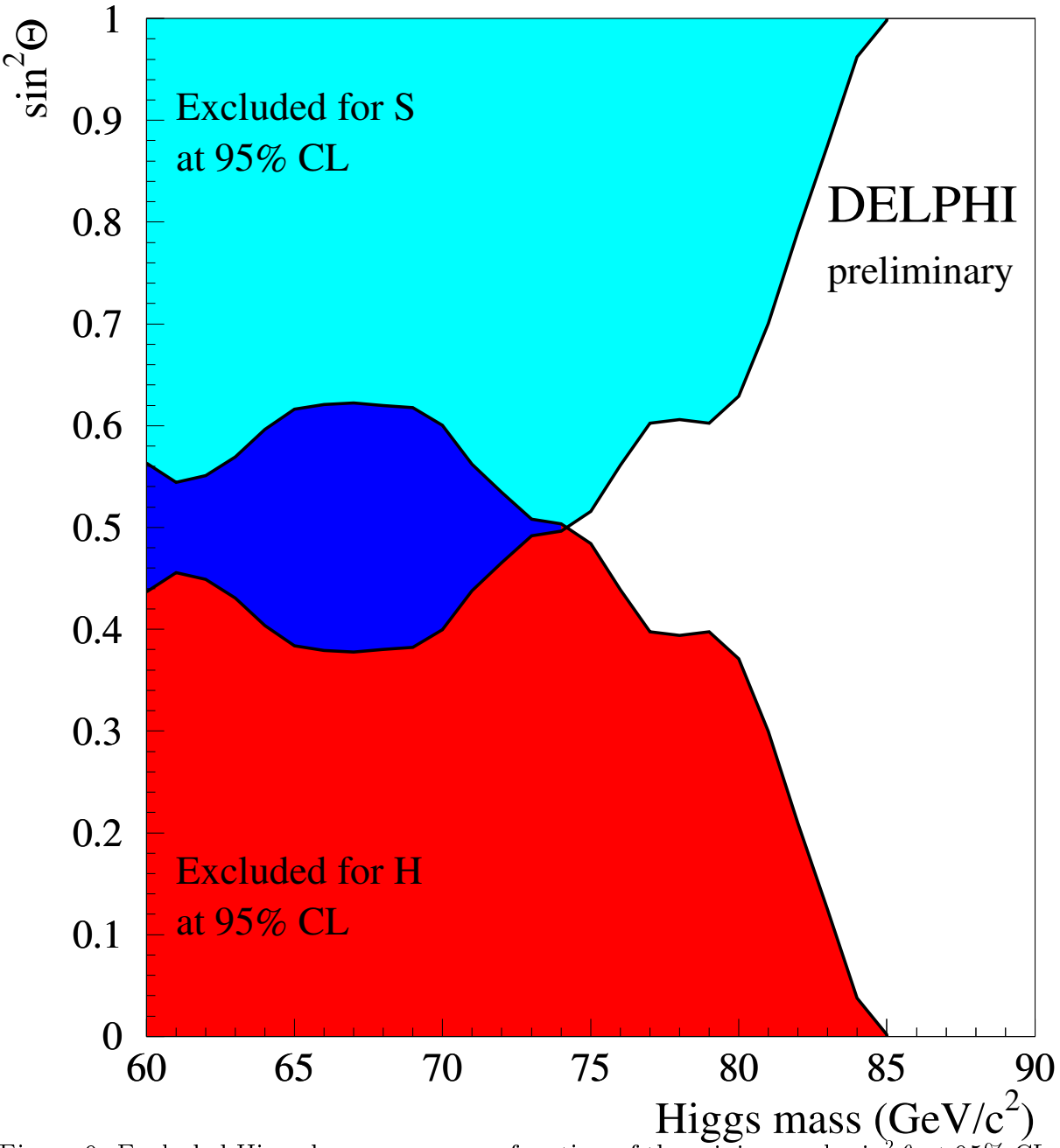

Figure 9: Excluded Higgs boson mass as a function of the mixing angle $\sin^2\theta$ at 95% CL. S and H are the Higgs bosons in the Majoron model with expected production rates for large $\tan\beta$. In this case, the Higgs decays only invisibly.

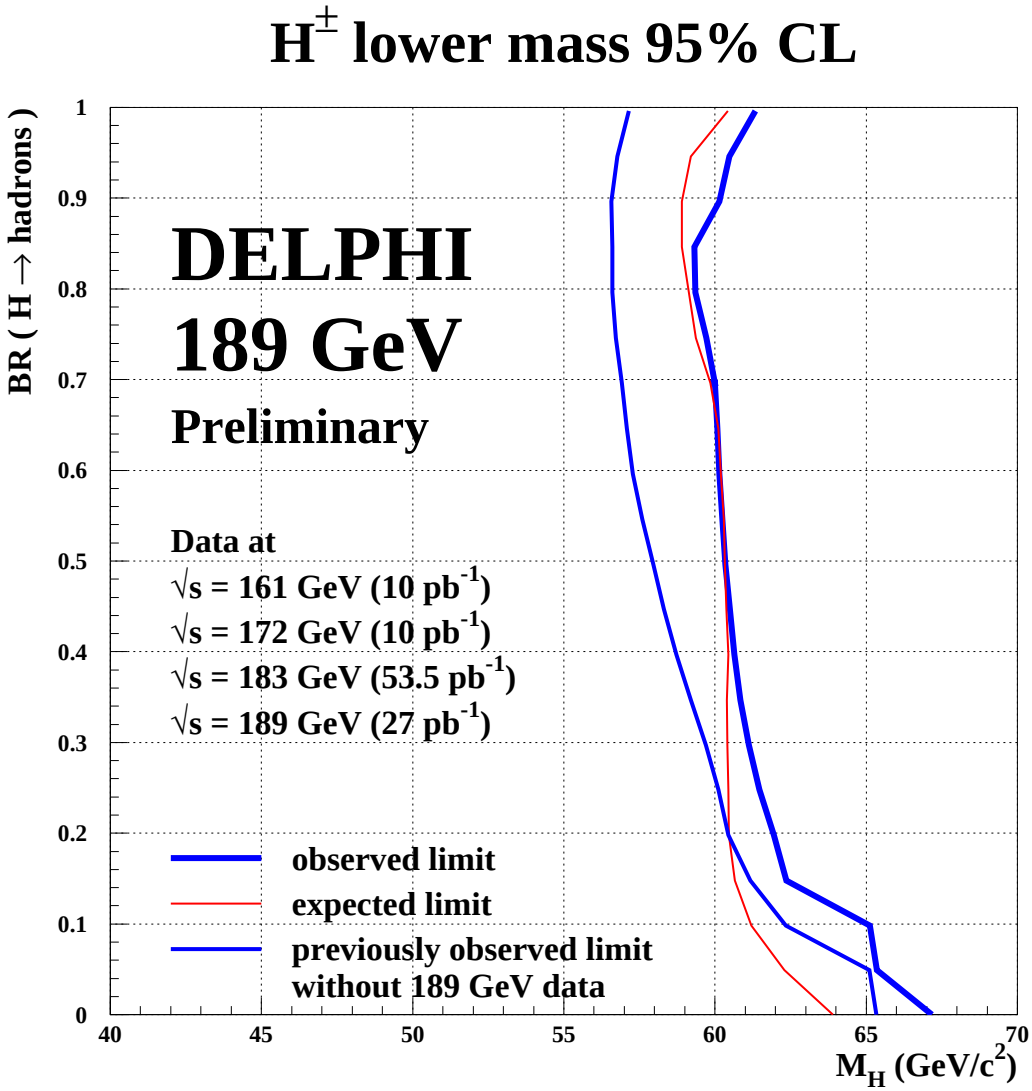

Figure 10: *The 95% confidence level observed and expected exclusion regions for $H^{\pm}$ in the plane BR(H $\longrightarrow$ hadrons) vs. $M_{H^{\pm}}$ obtained from a combination of the search results in the hadronic, semileptonic and leptonic decay channels at $\sqrt{s}$ = 161 GeV, 172 GeV, 183 GeV and 189 GeV.*

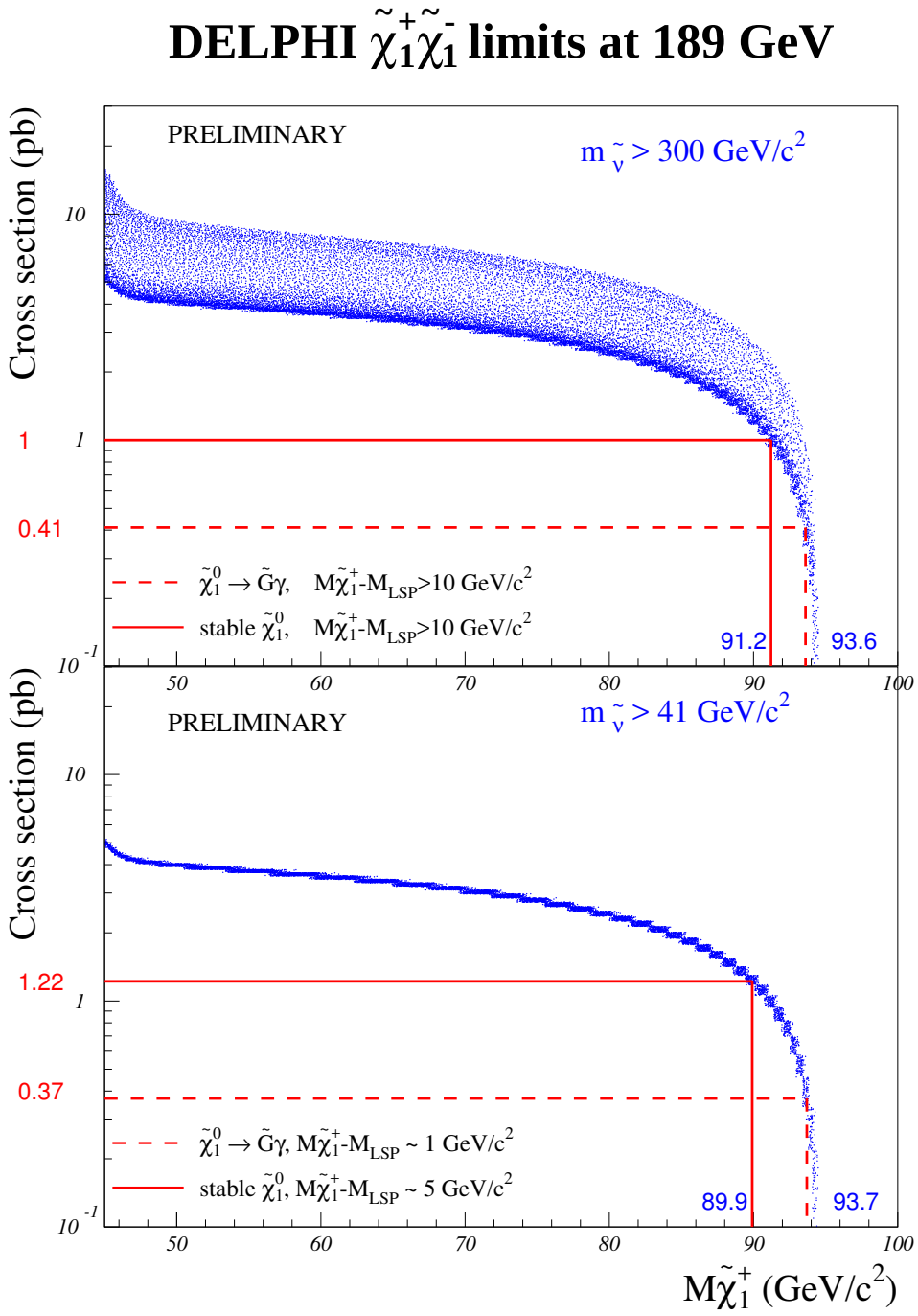

Figure 11: Expected cross-sections at 189 GeV (dots) versus the chargino mass in the non-degenerate scenario ($\Delta M > 10$ GeV/c^2) and in the degenerate scenario ($\Delta M \leq 5$ GeV/c^2), for different MSSM parameter values. A heavy sneutrino ($m_{\tilde{\nu}} > 300$ GeV/c^2) has been assumed in the upper plot and $m_{\tilde{\nu}} > 41$ GeV/c^2 in the lower one. The cross-sections indicated are the minimum ones in the excluded mass region.

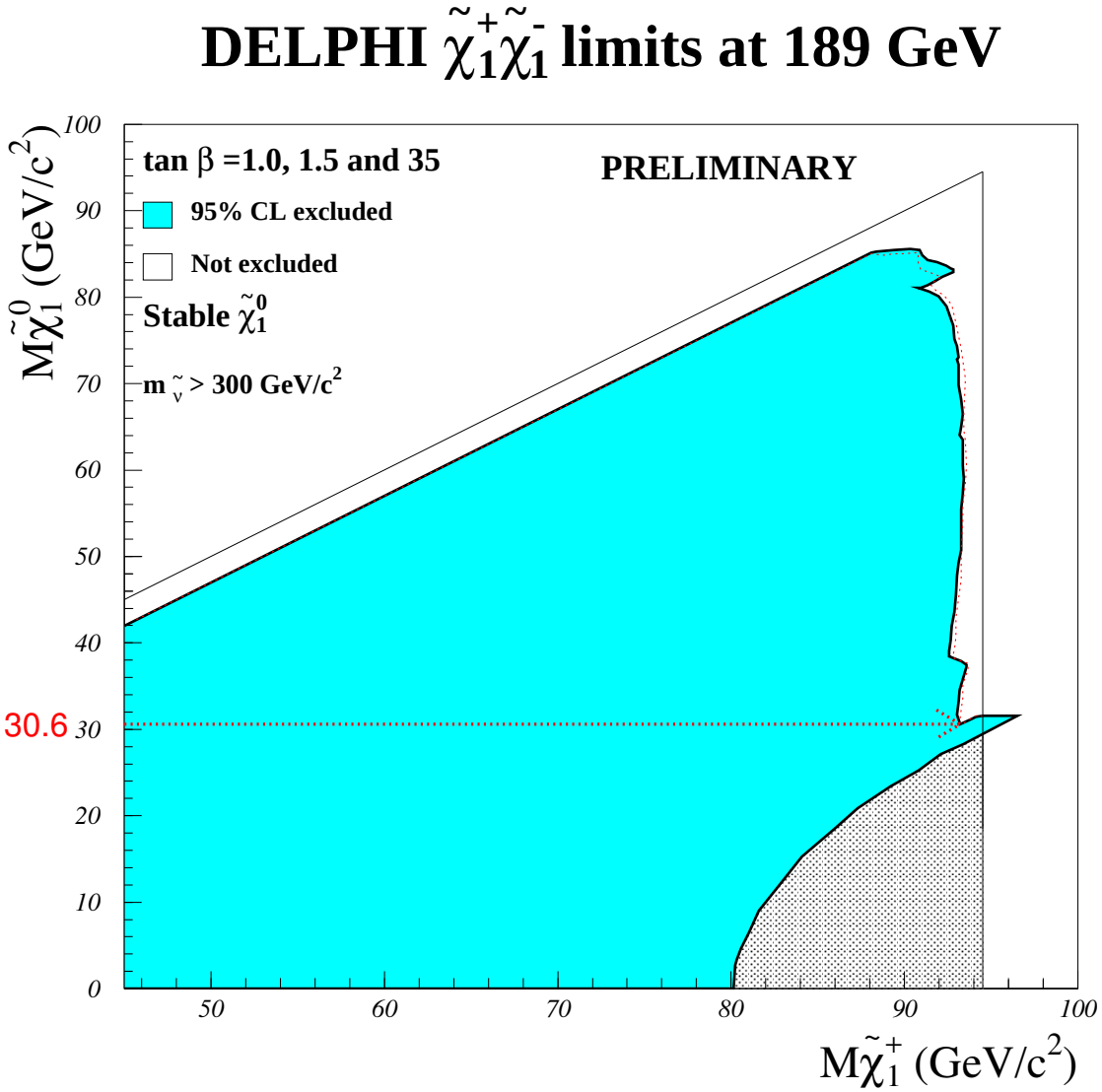

Figure 12: Regions excluded at 95% confidence level in the plane of the mass of the lightest neutralino versus that of the lightest chargino under the assumption of a heavy sneutrino. The thin lines show the kinematic limits in the production and the decay. The dotted line shows the expected exclusion limit. The lightly shaded region is not allowed in the MSSM. The limit applies in the case of a stable neutralino. The mass limit on the lightest neutralino is is then extracted looking for the minimal $M_{\tilde{\chi}_1^0}$ allowed by excluded region. The region which goes above the chargino kinematic limit is obtained using the limit on $\tilde{\chi}_1^0\tilde{\chi}_2^0$ production at the Z resonance derived from the single-photon search.

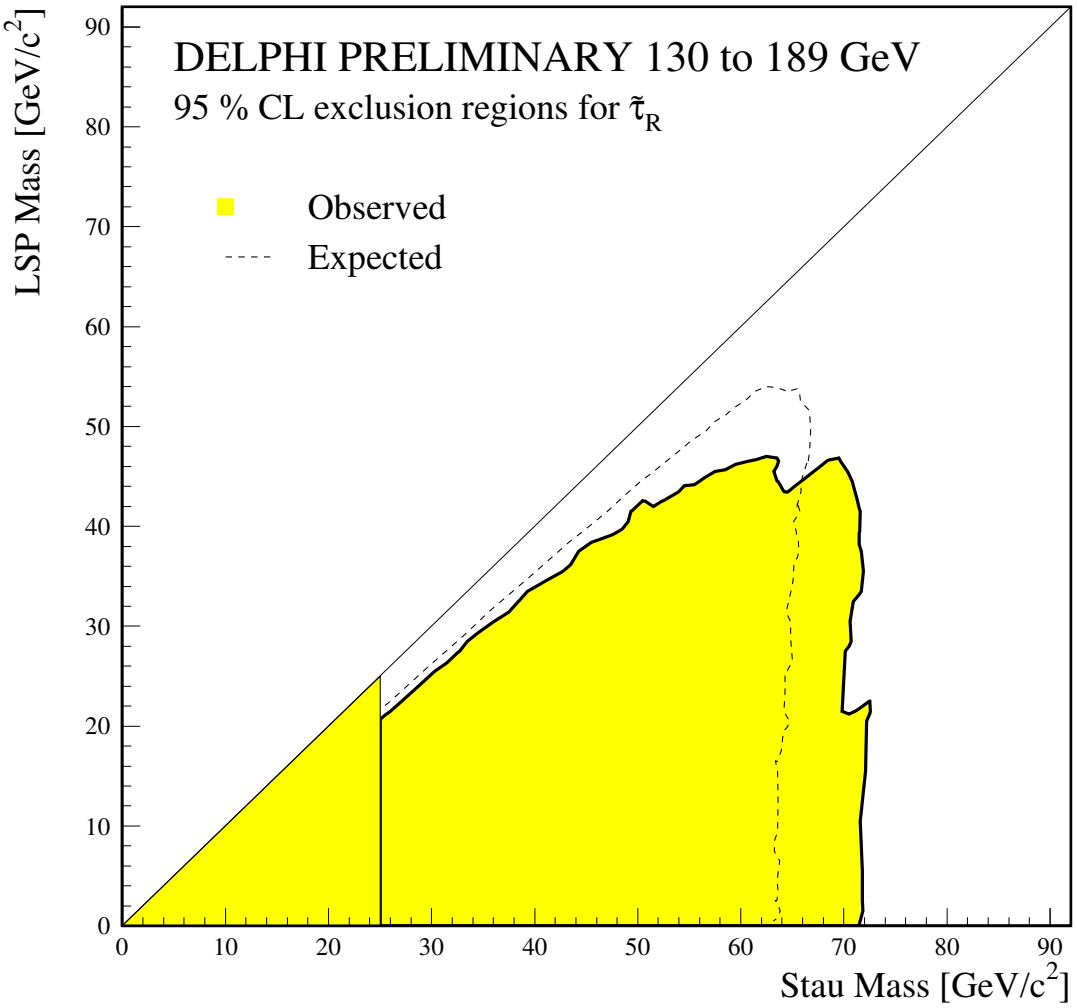

Figure 13: Exclusion limts at 95% confidence level for $\tilde{\tau}_R$. The full line represents the exclusion limit obtained and the dashed line the mean limit expected from background-only experiments.

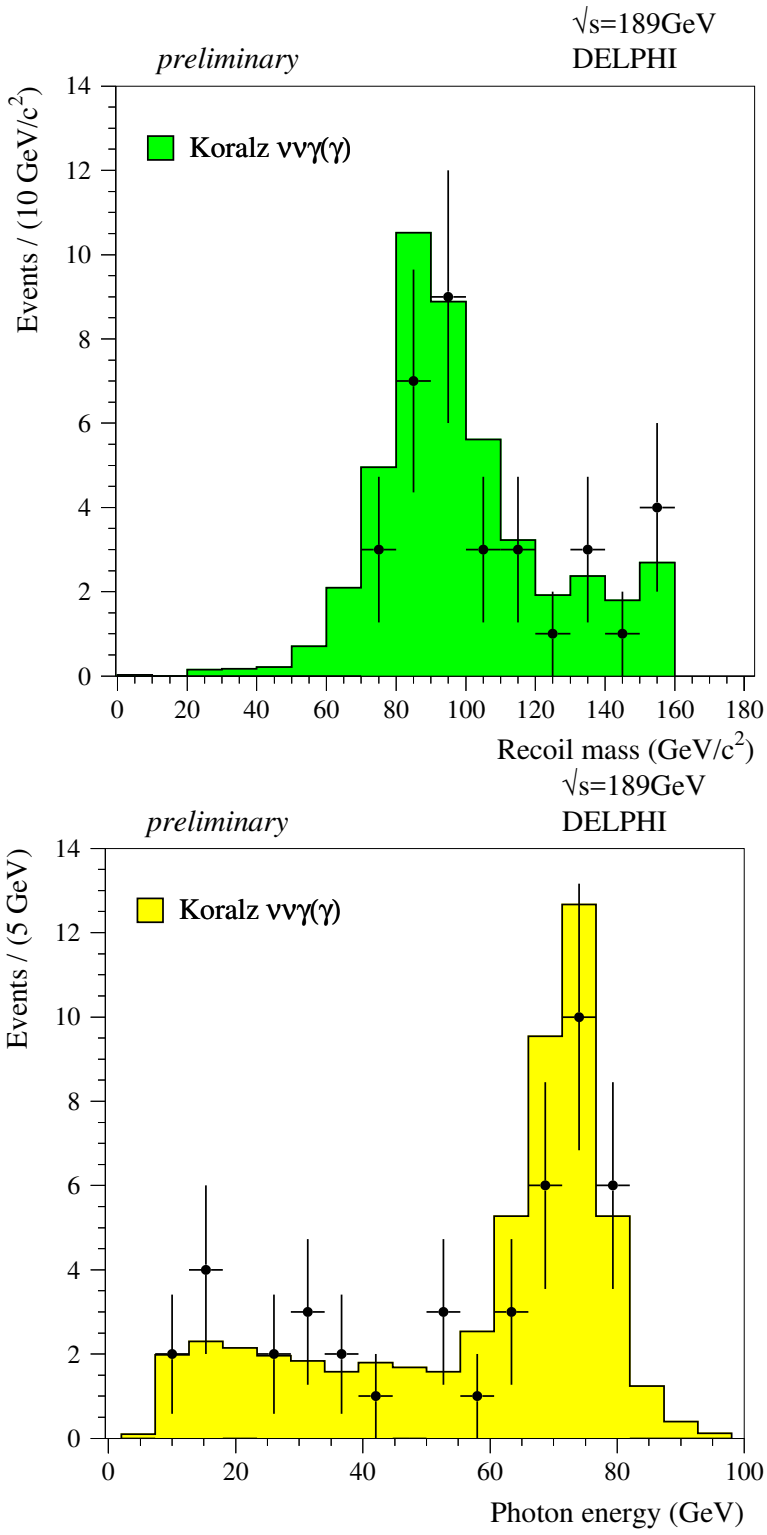

Figure 14: Photon recoil mass distribution (top) and energy spectrum (bottom) for the single-photon events collected at $\sqrt{s} = 189$ GeV.

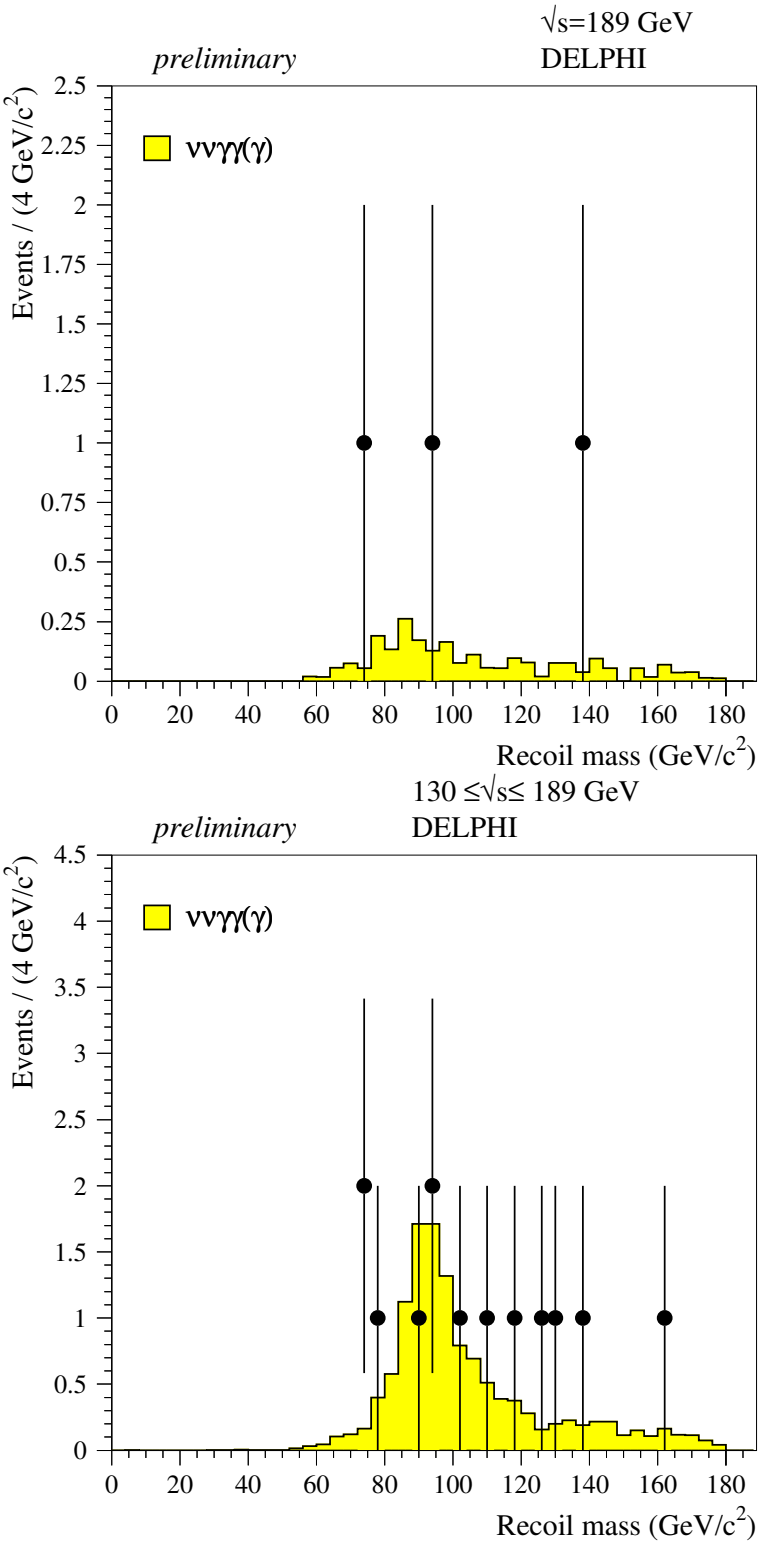

Figure 15: Missing mass distribution of the events passing the preselection at the centre-of-mass energy of 189 GeV (top) and summing up all centre-of-mass energies (bottom).

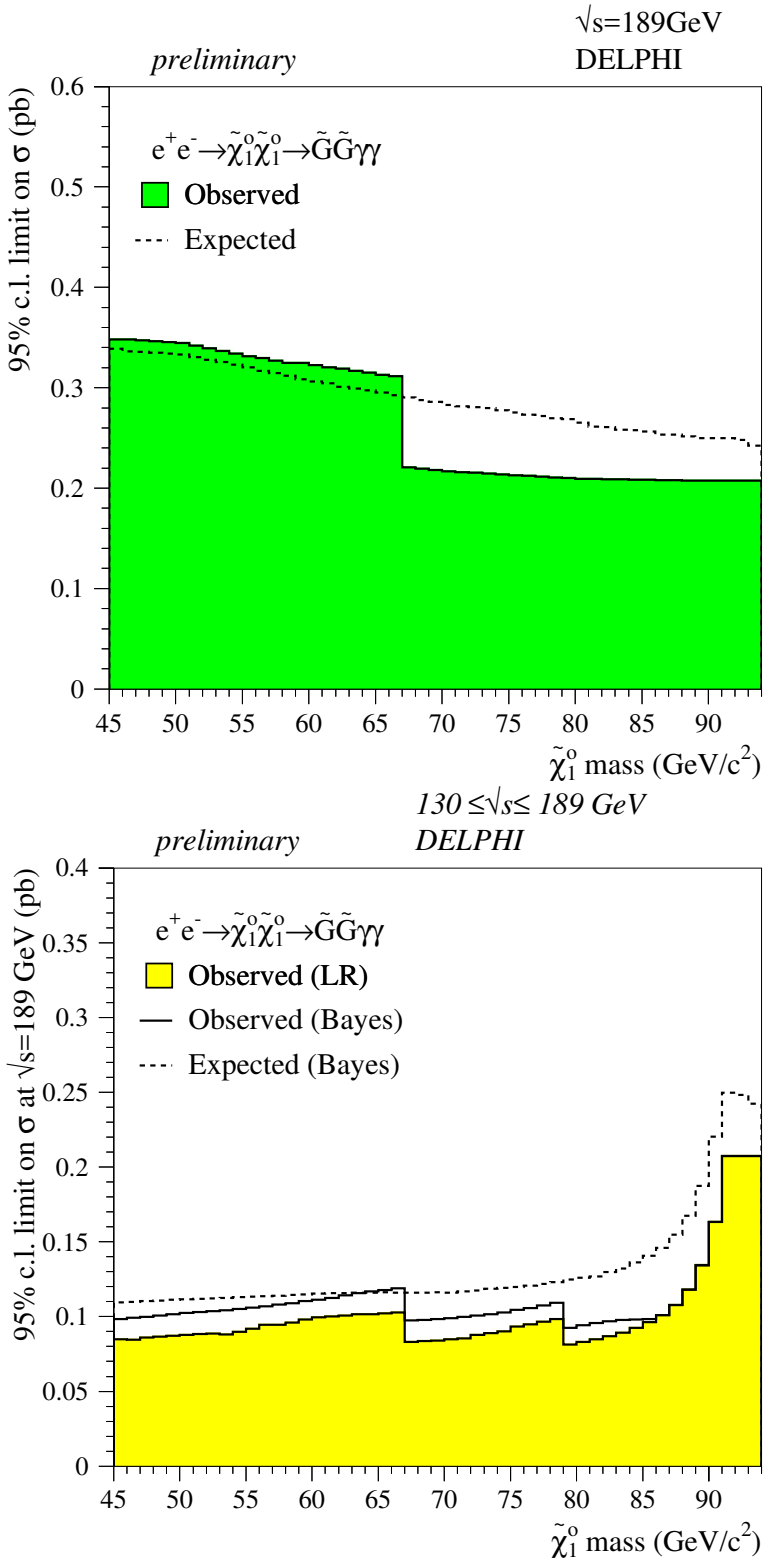

Figure 16: Upper limits at 95% confidence level on the cross-section for the process $e^+e^- \to \tilde{\chi}_1^0\tilde{\chi}_1^0 \to \tilde{G}\gamma\tilde{G}\gamma$ obtained from the data taken at $\sqrt{s} = 189$ GeV alone (top) and combining all the data samples collected at LEP2 (bottom). The limits assume BR($\tilde{\chi}_1^0 \to \tilde{G}\gamma$)=1. The limits apply for any generic process of the type $e^+e^- \to YY \to X\gamma X\gamma$ where X is a massless undetected particle.

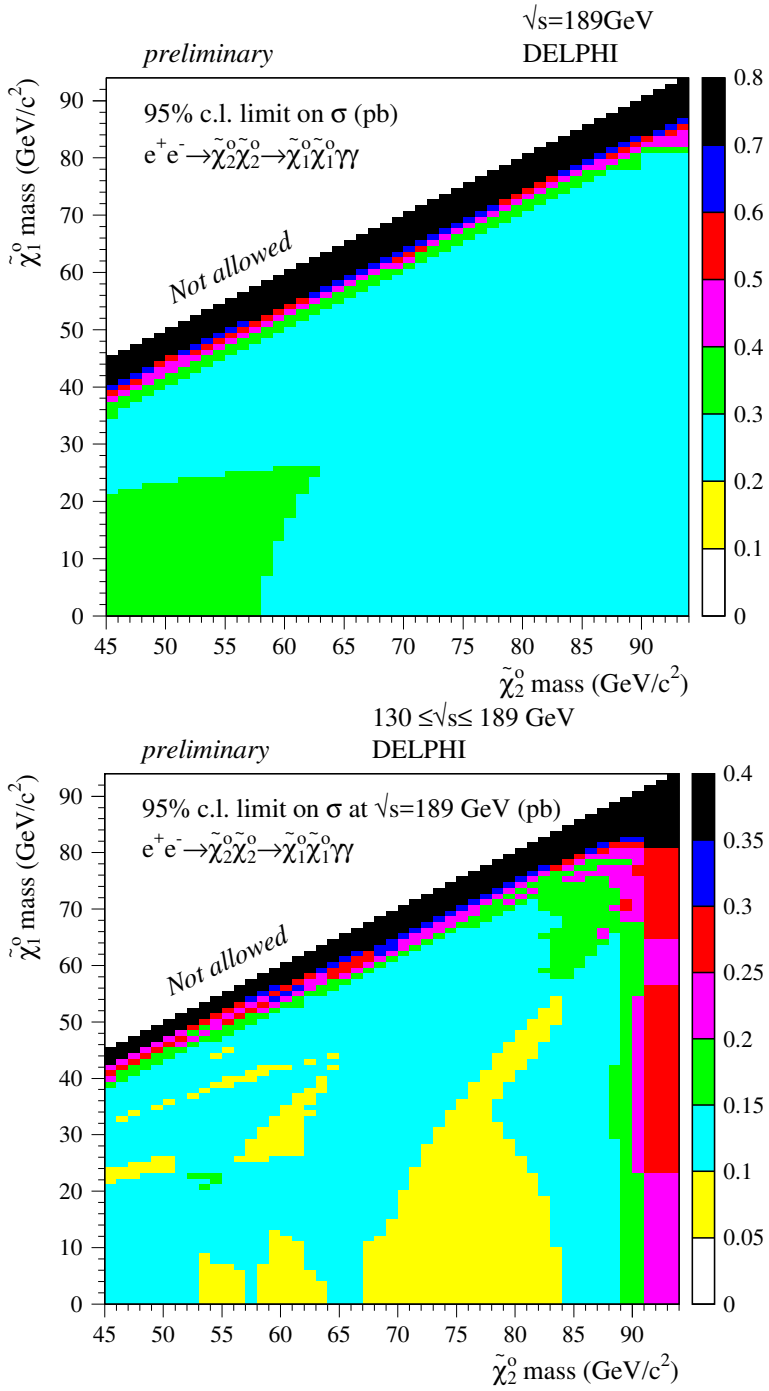

Figure 17: Upper limits at 95% confidence level on the cross-section for the process $e^+e^- \to \tilde{\chi}^0_2\tilde{\chi}^0_2 \to \tilde{\chi}^0_1\gamma\tilde{\chi}^0_1\gamma$ as a function of the $\tilde{\chi}^0_2$ and $\tilde{\chi}^0_1$ masses obtained using the data taken data at $\sqrt{s} = 189$ GeV alone (left) and combining all data samples collected at LEP2 (right). A 100% branching ratio is assumed for the decay $\tilde{\chi}^0_2 \to \tilde{\chi}^0_1\gamma$. The limits apply for any generic process of the type $e^+e^- \to YY \to X\gamma X\gamma$ where X is a massive undetected particle.

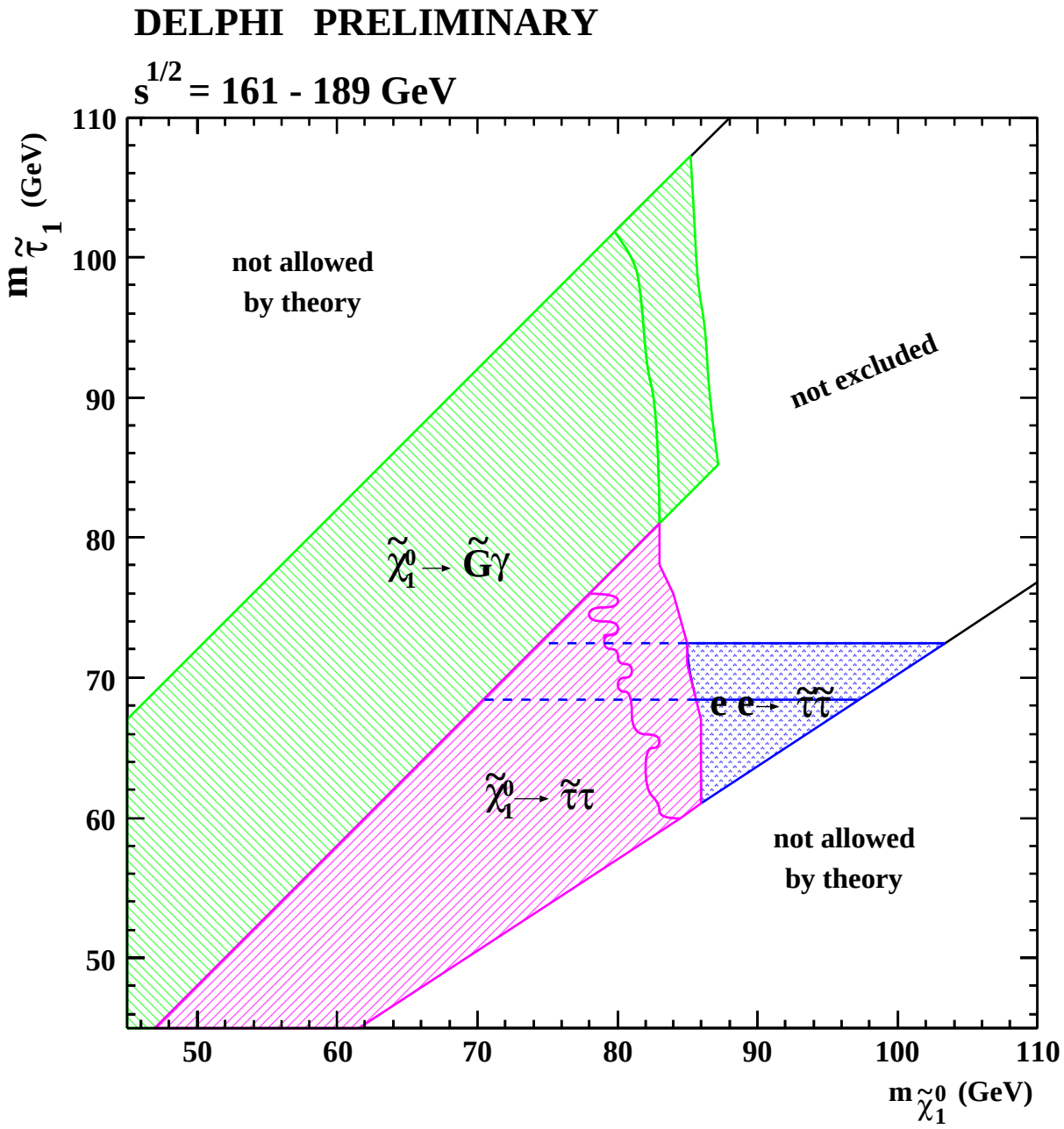

Figure 18: Areas excluded at the 95% CL for $n = 2$ and gaugino-like neutralinos in the $m_{\tilde{\chi}_1^0}$ *vs.* $m_{\tilde{\tau}_1}$ plane. The positive-slope dashed area is excluded by the extension of this analysis to 34 pb^{-1} at $\sqrt{s} = 189$ GeV. The negative-slope dashed area is excluded by the analysis searching for neutralino-pair production followed by the decay $\tilde{\chi}_1^0 \to \tilde{G}\gamma$. The pointed area is excluded by the direct search for MSSM $\tilde{\tau}_1$-pair production, taking into account the possibility of $\tilde{\tau}_L - \tilde{\tau}_R$ mixing [22].

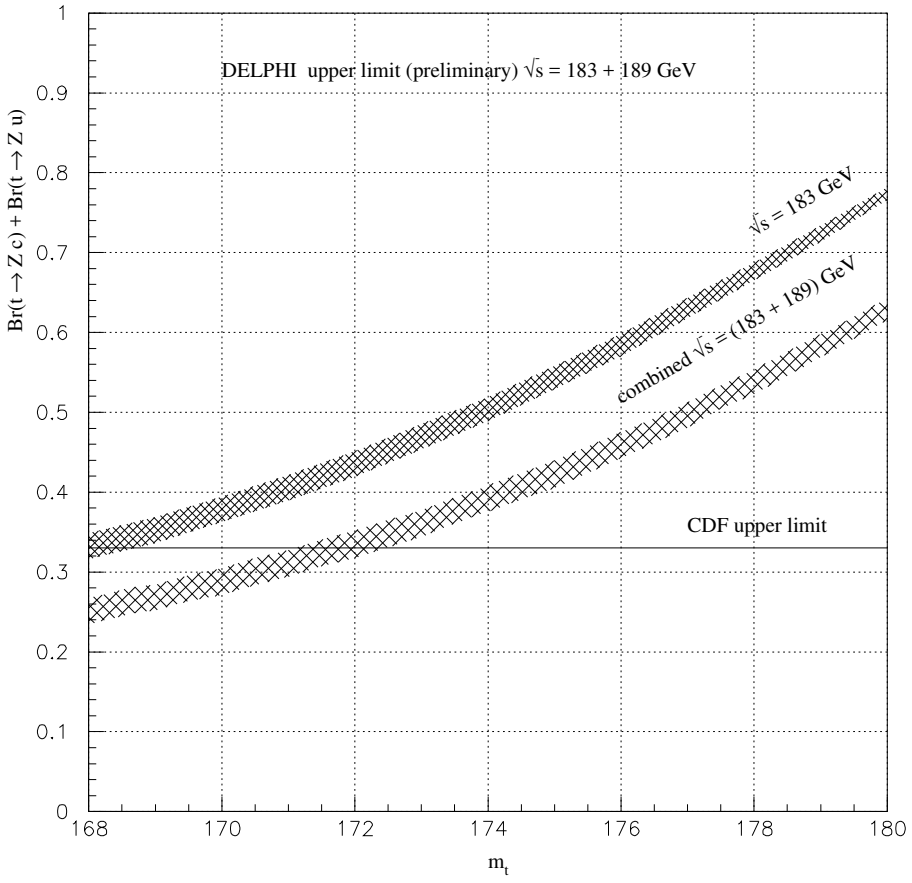

Figure 19: 90% confidence level upper limit on the branching ratio $Br(t \to Zc) + Br(t \to Zu)$ obtained from DELPHI at 183 GeV and by combining 183 and 189 GeV. Also shown is the CDF upper limit.